Single-mode low threshold current multi-hole vertical-cavity surface-emitting lasers*

Zhao Zhen-Bo(赵振波), Xu Chen(徐 晨)†, Xie Yi-Yang(解意洋), Zhou Kang(周 康), Liu Fa(刘 发), and Shen Guang-Di(沈光地)

Key Laboratory of Opto-electronics Technology of Ministry of Education, Beijing University of Technology, Beijing 100124, *China*

(Received 21 April 2011; revised manuscript received 5 June 2011)

A multi-hole vertical-cavity surface-emitting laser (VCSEL) operating in stable single mode with a low threshold current was produced by introducing multi-leaf scallop holes on the top distributed Bragg-reflector of an oxidation-confined 850 nm VCSEL. The single-mode output power of 2.6 mW, threshold current of 0.6 mA, full width of half maximum lasing spectrum of less than 0.1 nm, side mode suppression ratio of 28.4 dB, and far-field divergence angle of about 10° are obtained. The effects of different hole depths on the optical characteristics are simulated and analysed, including far-field divergence, spectrum and lateral cavity mode. The single-mode performance of this multi-hole device is attributed to the large radiation loss from the inter-hole spacing and the scattering loss at the bottom of the holes, particularly for higher order modes.

Keywords: single mode, low threshold current, multi-hole, vertical-cavity surface-emitting laser

PACS: 42.55.Px, 42.60.Jf, 42.62.Fi **DOI:** 10.1088/1674-1056/21/3/034206

1. Introduction

Single-mode vertical-cavity surface-emitting lasers (VCSELs) have attracted a lot of attention in recent years for their better beam quality and high efficiency coupling to optical fibers. They are important to free space optical interconnects, data communication through single mode fibers and modulation spectroscopy.[1−3] For these applications, VCSELs with stable single mode, lower threshold current and higher power are desirable. For oxide-confined VCSELs, the current-confined aperture must be less than 3 μm in diameter to ensure single-mode operation.[4] However, the large resistance inherited from the small oxide aperture limits the modulation bandwidth and speed. Furthermore, the lifetime and stability of the oxide VCSEL are related to the size of the oxide aperture. Therefore, several structures have been developed to obtain single-mode VCSELs with large oxide apertures, and these include increasing the higher order mode loss with a surface-relief structure,[5] and weakening the lateral cladding with a photonic crystal structure[2] and a triangular-hole structure.[6−8] The surface relief structure uses the selective loss concept, but the process of exact etching control is too hard to obtain. The photonic crystal structure provides weaker index guiding to obtain single mode,[9,10] but it is sensitive to heat effects. In this paper, a kind of multi-hole-structure VCSEL is produced and its performance is investigated. The deep-etched multi-leaf holey structure is used for higher order mode suppression.[11−13]

2. Simulation and experiment

2.1. Device model and simulation

Figure 1 is a schematic of the multi-leaf holey VCSEL device structure. The parameters are chosen as follows: the oxide aperture and emission aperture are 10 and 6 μm, respectively. There are eight leaf holes with an R of 8 μm and θ of 35°. In the simulation, the dipole optical source is located in the active region, and the electric and thermal effects are neglected.

Figures 2(a) and 2(b) show the far-field divergence angle dependence on the hole depths in the simulation and experiment, respectively. We can see that at hole depths of 1.2 and 2.4 μm, the far-field divergence angles are narrower, which agrees well with the experimental results, as shown in Fig. 2(b). The divergence angles from the experiment are broader than

*Project supported by the National High Technology Research and Development Program of China (Grant No. 2008AA03Z402), the National Natural Science Foundation of China (Grant No. 61076044), and the Natural Science Foundation of Beijing, China (Grant Nos. 4092007 and 4102003).

†Corresponding author. E-mail: xuchen58@bjut.edu.cn

© 2012 Chinese Physical Society and IOP Publishing Ltd

those from the simulation, which may be attributed to the electrical and thermal effects.

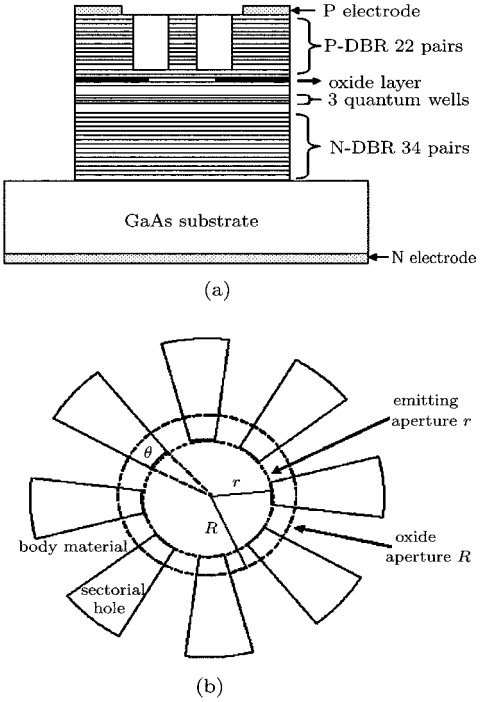


Fig. 1. (a) A cross-sectional view of the multi-leaf holey VCSEL device structure, and (b) the parameters of the multi-hole structure. DBR: distributed Bragg–reflector; R: radius of the oxide aperture; r: radius of the emitting aperture; θ: angle of the scallop holes.

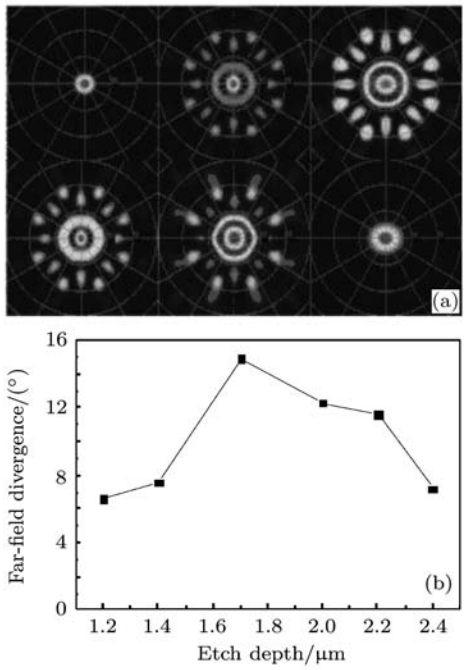


Fig. 2. Simulation results of the far-field divergence angle dependence on hole depth: (a) simulation results (the depths, from left to right, top to bottom, are 1.2, 1.4, 1.7, 2.0, 2.2, and 2.4 μm, respectively); (b) experimental results.

Figure 3 shows the spectrum dependence on hole depth in the simulation. We can find that the side mode suppression ratios (SMSRs) are much higher when the hole depths exceed 2.0 μm.

Figures 4(a) and 4(b) show the simulation results of the resonant cavity modes of conventional oxide-confined VCSELs and multi-hole VCSELs, respectively. When we introduce multi holes on the top DBR of the VCSEL, we realize single-mode lasing, as shown in Fig. 4(b).

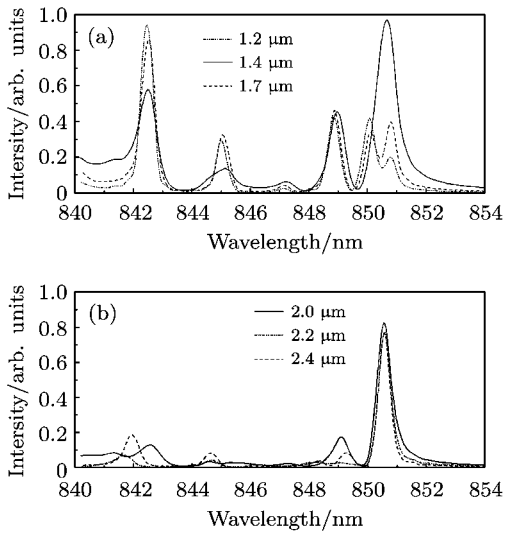


Fig. 3. The spectrum of different depth holey VCSELs: (a) with hole depths of 1.2, 1.4, and 1.7 μm; and (b) with hole depths of 2.0, 2.2, and 2.4 μm.

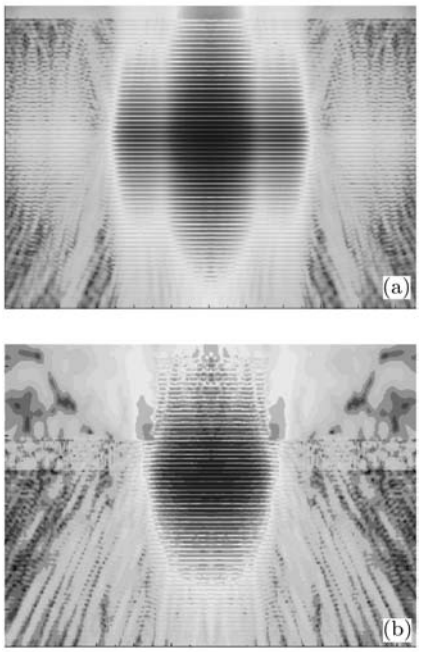


Fig. 4. (a) The resonant cavity modes of oxidized VCSELs, and (b) the resonant cavity modes of multi-hole VCSELs.

2.2. Device structure and fabrication

The multi-hole VCSEL was produced by etching holes on the top DBR of a conventional VCSEL. The conventional VCSEL was fabricated from a 3 inch n-type wafer with an epitaxial structure consisting of a bottom n-type (Si-doped) 34 pair DBR, an undoped active region with three GaAs quantum wells, and a similar top (C-doped) 22 pair DBR. The DBRs are formed by the graded heterojunction of $Al_xGa_{1-x}As$, the unit period of bottom and top DBR mirrors consisting of four layers of $Al_xGa_{1-x}As$ (x: is from 0.9 to 0.12), $Al_{0.12}Ga_{0.88}As$, $Al_xGa_{1-x}As$ (x is from 0.12 to 0.9), and $Al_{0.9}Ga_{0.1}As$. In addition, a 30 nm $Al_{0.99}Ga_{0.02}As$ oxidization layer was inserted between the top DBR and the active region.[2] The operation wavelength of the device is designed at 850 nm.

The circular mesas were formed by $SiCl_4/Ar/Cl_2$ inductively coupled plasma reaction ion etching (ICP-RIE) down close to the active region, using SiO_2 as the etching mask. Then the $Al_{0.99}Ga_{0.02}As$ layer was selectively oxidized to form the oxide aperture with a diameter of 10 μm to confine the spread of current. After that, top ohmic (Ti/Au) ring contacts were patterned and bottom ohmic (AuGeNi/Au) contacts were formed. Then the devices were annealed by rapid thermal annealing at 430 °C for 35 s, and the process of a conventional VCSEL was finished.

With the simulation instructions, we chose a hole depth of about 2.4 μm, an oxide aperture of about 10 μm and an optical aperture of about 6 μm. On the top of the conventional VCSEL, eight scallop holes were patterned using electron beam lithography and transferred into top DBR using $SiCl_4/Ar/Cl_2$ ICP-RIE. Figure 1(b) shows the structural characteristics of the multi-holes. In this work, the multiple holes are arranged around the oxide aperture and the lateral penetration of the scallop hole into the oxide aperture (R–r) is about 2–3 μm, resulting in an emitting aperture ($2r$) of about 6 μm. The angle θ and radius r of the scallop holes are 35°, 6–8 μm, respectively, and the etching depth is 2.4 μm, corresponding to about 80% of the top DBR. The cross-sectional diagram of the multi-hole VCSEL is shown in Fig. 1(a).

3. Results and discussion

The continual wave current output characteristics of the devices were tested at room temperature. Figure 5 shows the power–current and current–voltage characteristics of the multi-hole VCSEL. The device exhibits a threshold current of 0.6 mA, a maximum output power of 2.6 mW and a series resistance of 75 Ω.

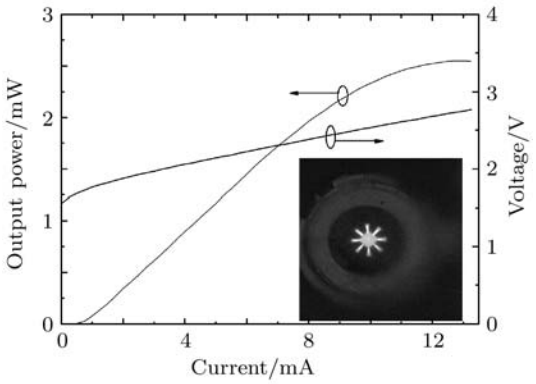


Fig. 5. The light output power and voltage versus injection current of the multi-leaf holey VCSEL.

Figures 6(a) and 6(b) show the far-field distribution of the multi-hole VCSEL and the conventional VCSEL with the same oxidation aperture of 10 μm at an injection current of 10 mA. The divergence angle of the conventional VCSEL is more than 20°, with two peaks in both the horizontal and vertical directions, indicating that it is operating in multi-transverse modes. In contrast, the far-field divergence angle of the multi-hole VCSEL is less than 10°, and has only one peak in the two directions.

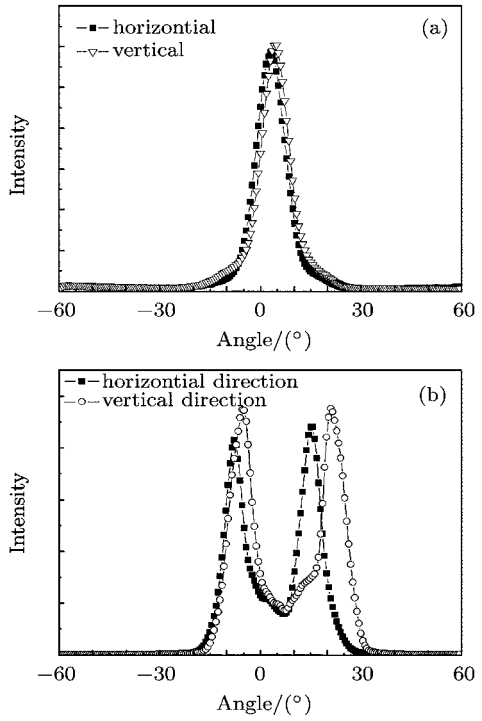


Fig. 6. The far-field divergence angle of (a) the multi-leaf holey VCSEL with eight holes, and (b) the conventional VCSEL with the same oxidation aperture size at the same injection current.

Figures 7(a) and 7(b) show the spectrum characteristics of the multi-hole VCSEL and oxidized VCSEL, respectively. The optical spectrum of the conventional VCSEL is wide and has many intensity peaks with a full width at half maximum (FWHM)

of more than 1 nm. The multi-hole VCSEL has wonderful optical spectrum characteristics, showing only one main peak with an FWHM of less than 0.1 nm and a side-mode suppression ratio (SMSR) of 28.4 dB throughout the whole current operating range. Both the far-field distribution and the optical spectrum have showed effective mode controlling of the multi-hole structure.

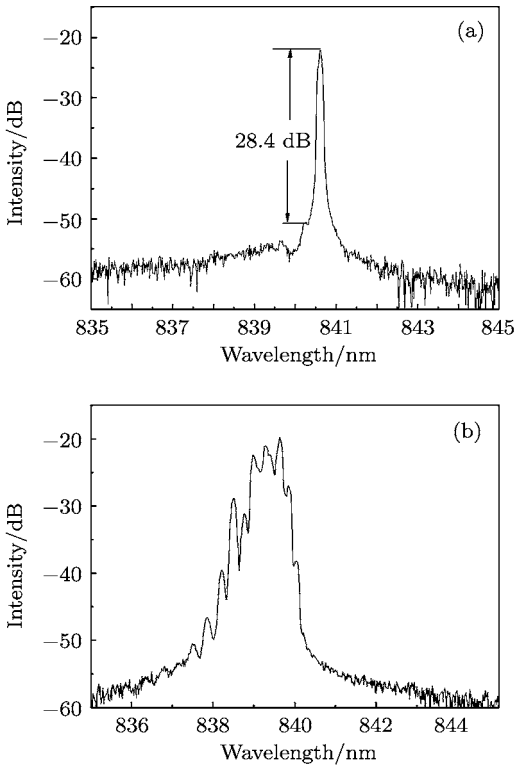


Fig. 7. (a) The spectrum characteristics of the multi-hole VCSEL, and (b) the spectrum characteristics of the oxidized VCSEL with the same operational current and oxidized aperture size. The injection current is 10 mA.

The multi-hole VCSEL shows excellent single-mode performance and lower threshold current owing to the optimal design of the holey structure. In order to reduce the threshold current, the oxide aperture should also be reduced. However, the emitting aperture must be smaller than the oxide aperture, so the oxide aperture cannot be too small to obtain enough output power. Moreover, a small oxide aperture will lead to excessive series resistance, causing instable work status. Therefore, the oxide aperture should be chosen properly. On the other hand, if the dimension of the emitting aperture is too close to that of the oxide aperture, the scallop-hole structure cannot control the mode performance effectively, and in order to obtain higher output power, it cannot be much smaller than the oxide aperture. The etching depth of the scallop holes is also important for mode control. A scallop-hole structure with an improper shallow etching depth can obtain narrow far-field divergence, but cannot control the transverse mode and spectrum effectively. A large enough etching depth but that does not damage the active region is necessary. In short, the parameters of the multi-hole structure should be carefully chosen to obtain better performance, including higher single-mode power, lower threshold current and series resistance.

4. Conclusion

In summary, a multi-hole structure can be used to control the mode performance of VCSELs effectively. VCSELs with excellent single-mode performance, narrow far-field divergence, higher SMSR, low threshold current and series resistance can be realized by appropriately choosing the multi-scallop-hole structure parameters.

References

[1] Song G F, Zhang Y, Guo B S and Wang W M 2009 *Acta Phys. Sin.* **58** 7278 (in Chinese)

[2] Xie Y Y, Xu C, Kan Q, Wang C X, Liu Y M, Wang B Q, Chen H D and Shen G D 2010 *Chin. Phys. Lett.* **27** 024206

[3] Chen C, Leisher P O, Kuchta D M and Choquette K D 2009 *IEEE Journal of Selected Topics in Quantum Elcecronics* **15** 673

[4] Weigl B, Grabherr M, Michalzik R, Reiner G and Ebeling K J 1997 *IEEE Photonics Technol. Lett.* **8** 971

[5] Haglund Å, Gustavsson J S, Vukušić J, Modh P and Larsson A 2004 *IEEE Photonic Technol. Lett.* **16** 368

[6] Furukawa A, Sasaki S, Hoshi M and Matsuzono A 2004 *Appl. Phys. Lett.* **85** 5161

[7] Furukawa A, Hoshi M and Sasaki S 2005 *Proc. SPIE* **183** 5722

[8] Liu A J, Qu H W, Chen W, Jiang B, Zhou W J, Xing M X and Zheng W H 2011 *Chin. Phys.* B **20** 024204

[9] Xu Y Z, Ren X M, Zhang X and Huang Y Q 2006 *Chin. Phys. Lett.* **2309** 2759

[10] Noriyuki Y, Danner A J and Choquette K D 2003 *Appl. Phys. Lett.* **82** 91344

[11] Yang H P D, Liu J N, Yeh Z E, Lai F I, Lee T D, Kuo H C and Chi J Y 2008 *J. Modern Opt.* **55** 341

[12] Liu A J, Chen W, Qu H W, Jiang B, Zhou W J, Xing M X and Zheng W H 2010 *Laser Phys. Lett.* **7** 213

[13] Wang S H, Ren L Y and Liu Y 2009 *Acta Phys. Sin.* **58** 3943 (in Chinese)